Robot Path Planning for Spray Coating: A Frequency Domain Approach

Stephen Duncan, Paul Jones and Peter Wellstead

Abstract— **Most modern spray deposition processes, such as spray painting or coating, are automated by using a robot to move an applicator over the surface being sprayed. Determining the robot path that creates the required coat thickness over the surface can be considered as an optimisation problem, which traditionally has been solved in the spatial domain. In this paper, results from sampling theory are used to transfer the problem into the spatial frequency domain. These results are used to determine the optimal path for a spraying application. The paper also shows how angled raster patterns can be combined to provide a continuous path over the surface that generates the required distribution of deposited material.**

I. INTRODUCTION

In most automated spray deposition processes, such as spray painting, metal spray deposition and coating, an applicator is moved over the surface being sprayed by a robot. Usually, a key quality variable is the coat thickness, which is required to match a desired profile over the surface and the path taken by the robot needs to be chosen so that this desired profile is achieved. Choosing the optimal path can be considered as an optimisation problem [1], [12], [2], [3], [10], [9], [14]. It is recognized that solving the full optimisation problem is difficult and as a result, a number of sub-optimal solutions have been presented. However, in the previously published literature, the optimisation problem is solved in the spatial domain. In this paper, the optimisation problem is transferred to the spatial frequency domain by using results from sampling theory [11]. Although it is not claimed that this provides better or more efficient solutions to the optimisation problem, it does provide valuable insight into the choice of factors such as the separation between the applicator's passes over the surface, by providing a direct link between the Fourier transform of the spray footprint and the path separation. It also shows how angled raster patterns can be combined to provide a continuous path over the surface that generates the required distribution of deposited material.

The paper is laid out as follows. Section II describes a model of the spraying process and lays out the optimisation problem. Section III shows how the problem can be converted to the spatial frequency domain by considering it as a sampling problem. Section IV uses these results to determine the optimal path for a spraying application.

This work was supported by the UK Engineering and Physical Research Council under grant GR/M87832 and the Ford Motor Corporation.

S. Duncan and P. Jones are with the Department of Engineering Science, University of Oxford, Oxford OX1 3PJ, United Kingdom. stephen.duncan@eng.ox.ac.uk paul.jones@bnc.ox.ac.uk

P. Wellstead is with the Hamilton Institute, National University of Ireland, Maynooth, Eire. peter.wellstead@may.ie

II. PROBLEM STATEMENT

Using cartesian coordinates, define the surface being sprayed as $z = h(x, y)$, where $(x, y) \in \mathcal{D}$ denotes the domain of the surface and the height, z, of the surface is determined from the location (x, y) [1]. The location and orientation of the applicator at time t can be described by the six-element vector

$$\mathbf{p}(t) = [x_a(t)\ y_a(t)\ z_a(t)\ a(t)\ b(t)\ c(t)]^T \qquad (1)$$

where $x_a(t)$, $y_a(t)$ and $z_a(t)$ represent the location of the applicator in cartesian space and $a(t)$, $b(t)$ and $c(t)$ refer to the rotation of the applicator relative to the X, Y and Z axes. The evolution of $\mathbf{p}(t)$ over time defines the path taken by the robot as it moves the applicator over the surface.

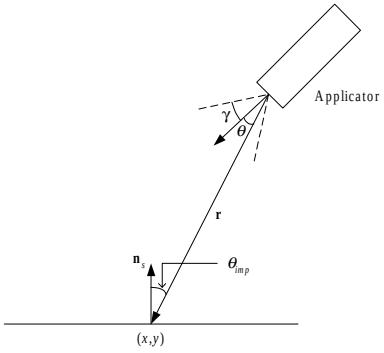

Fig. 1. Arrangement of applicator for deposition model in (2)

When the applicator is at a specific location, $\mathbf{p}(t)$, the rate of deposition at the point $(x, y, h(x, y))$ on the surface can be written as $f_s(\mathbf{p}(t), x, y)u(t)$, where $f_s(\mathbf{p}(t), x, y)$ denotes the spray "footprint" and $u(t)$ denotes the flow rate from the applicator. It is assumed that the flow rate, $u(t)$, is a variable that can be adjusted as the applicator moves over the surface. The footprint, $f_s(\mathbf{p}(t), x, y)$, depends upon the distance from the applicator to the surface and upon its orientation in space. In this analysis, we use the experimentally determined model for the rate of deposition (measured in kg m^{-2}) at the point (x, y) on the surface, which was determined by measuring the distribution of mass deposited over a known time period by the applicator positioned in a single fixed position and then solving the inverse problem to

determine the flow rate distribution [6]. When the applicator is located at $\mathbf{p}(t)$, the flow rate distribution is modelled as

$$f_s(\mathbf{p}(t), x, y) = \frac{\cos(\theta_{imp})\Theta(\theta, \gamma)\zeta(\theta_{imp})}{|\mathbf{r}^2|} \tag{2}$$

where as shown in Fig. 1, $\mathbf{r}$ is the vector from the applicator to the point (x, y), θ_{imp} is the impact angle between $\mathbf{r}$ and the surface normal, $\mathbf{n}_s$ at (x, y), and $\Theta(\theta, \gamma)$ describes the distribution of droplets within the spray cone. The droplet distribution is modelled as a regularised Dirac function that depends upon θ, the angle between the applicator normal (determined by its orientation), and γ, the half angle of the spray cone

$$\Theta(\theta, \gamma) = \frac{(\gamma^2 - \pi^2)\left[1 + \cos\left(\frac{\pi\theta}{\gamma}\right)\right]}{2\pi[2\gamma^2 - \pi^2 + \pi^2\cos\gamma]} \tag{3}$$

For the spray applicator used in this process, γ was found to be 0.32 radians. In some spraying (particularly in metal spraying), a significant portion of the sprayed material is lost due to splashing and the term $\zeta(\theta_{imp})$ describes the sticking efficiency at the point (x, y)

$$\zeta(\theta_{imp}) = \zeta(0)\left[1 - \alpha\theta_{imp}^2\left(1 - \frac{2\theta_{imp}^2}{\pi^2}\right)\right] \tag{4}$$

where $\zeta(0)$ is the sticking efficiency at normal incidence, which is measured to be 0.67, and $\alpha = 0.04$ is a fitting parameter. Note that in this model, there is no material deposited outside the region of the spray cone defined by the angle, γ. In practice, some of the splashed material will land on the surface and be deposited and although this can be modelled [6], it is not considered here. Fig. 2 shows the footprint for this applicator when spraying normally onto a flat surface.

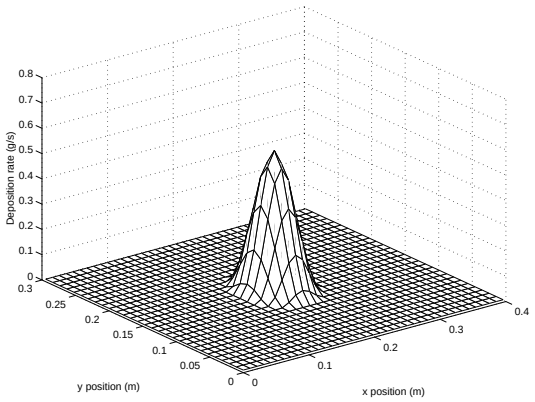

Fig. 2. Footprint of mass deposition from gun model in (2)

The aim is to deposit a pre-determined distribution of material, $m(x, y)$, over the surface. In principle, $m(x, y)$ can vary over the surface, but in practice, most applications require an even distribution of material, so that $m(x, y)$ equals a constant value. The problem is to determine, $\mathbf{p}(t)$, the path and orientation of the applicator as it is moved over the surface, together with the flow rate, $u(t)$, that will achieve this desired distribution. If the objective is to minimise the variance between the desired and achieved distributions [1], then the optimisation problem can be expressed as

$$\min_{\mathbf{p}(t), u(t)} \int_{\mathcal{S}} \left| m(x, y) - \int_0^T f_s(\mathbf{p}(t), x, y)u(t)dt \right|^2 dxdy \tag{5}$$

where $\mathcal{S}$ denotes the surface, such that $(x, y) \in \mathcal{S}$, and T denotes the time taken to complete movement of the applicator over the surface. It is difficult to solve this optimisation problem as it stands, primarily because the objective function is non-convex [1], [14]. For this reason, in this paper, we consider a simpler optimisation, where the surface to be sprayed remains flat, so that $h(x, y)$ is constant, and the applicator is oriented so that it remains normal to the surface and is held at a constant distance from the surface. Under these circumstances, the robot path is determined solely by $x_a(t)$ and $y_a(t)$ and the shape of the spray footprint does not change as the applicator is moved over the surface, so that

$$f_s(\mathbf{p}(t), x, y) = f(x - x_a(t), y - y_a(t)) \tag{6}$$

where $f(x - x_a(t), y - y_a(t))$ denotes the constant spray footprint when positioned at $(x_a(t), y_a(t))$. Choosing the optimal spray path and/or the optimal applicator velocity has been considered by a number of authors, including [12], [13], [10], [14]. In some of these papers, it is assumed that the applicator velocity can be adjusted, but in this paper, we assume that the applicator velocity remains fixed, but the flow rate $u(t)$ can be adjusted. The aim is therefore to solve

$$\min_{x_a, y_a, u} \int_{\mathcal{S}} \left| m(x, y) - \int_0^T f(x - x_a(t), y - y_a(t))u(t)dt \right|^2 dxdy \tag{7}$$

III. CONSIDERING SPRAYING AS SAMPLING PROCESS

Initially, we consider the case where the applicator follows the "raster" pattern shown by the solid line in Fig. 3 (the rationale behind this choice of path will be given below). The path consists of set of straight, parallel passes over the surface, connected by short straight sections at right angles to the main passes, where these short sections are made at a distance beyond the edge that is larger than the width of the spray cone shown in Fig. 2. This ensures that the spray does not contribute to these material deposited on the part when the applicator is following these sections of the path. For simplicity, it is assumed that a rectangular part is being sprayed, although the analysis is equally applicable to other shaped parts, provided that they are flat.

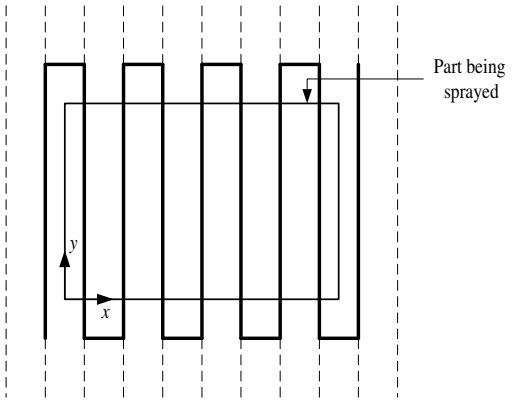

Fig. 3. Raster spray pattern. The actual spray path is shown by the solid line. The dashed lines show the extensions to $\pm\infty$

The time dependence on the spray footprint, $f(x - x_a(t), y - y_a(t))$, comes from the movement of the applicator over the surface. For the path in Fig. 3, the location of that applicator along each straight parallel section, where the applicator is spraying onto the part, can be described by

$$y_a(t) = vt + c \tag{8}$$

where v is the constant velocity of the applicator as it moves over the surface and c is a constant equal to the cumulative distance that the applicator has moved before the start of each raster scan. For this path, the time dependence on the flow rate, can be written as a function of the applicator position, $u(x_a, y_a)$ and the minimisation in (7) becomes

$$\min_{x_a, y_a, u} \int_{\mathcal{S}} \left| m(x,y) - \sum_{\text{paths}} \int_0^L f(x - x_a, y - y_a) u(x_a, y_a) \frac{1}{v} dy_a \right|^2 dxdy \tag{9}$$

where $0 \leq y_a \leq L$ denotes the path. Since $u(x_a, y_a)$ is only defined along the path, then it can be considered as being zero for all other values of (x, y), and the optimisation problem can be written

$$\min_{x_a, y_a, u} \int_{\mathcal{S}} \left| m(x,y) - \frac{1}{v} f(x,y) * u(x,y) \right|^2 dxdy \tag{10}$$

where $*$ denotes the convolution

$$f(x,y) * u(x,y) = \int_{\mathcal{S}} f(x - x_a, y - y_a) u(x_a, y_a) dx_a dy_a \tag{11}$$

Assume that the desired profile can be extended beyond the boundaries of the surface, so that $m(x, y)$ is defined on $\{x \in (-\infty, \infty), y \in (-\infty, \infty)\}$ (this assumption will be relaxed below), then using Rayleigh's theorem [4], the problem can be expressed in the spatial frequency domain

$$\min_U (\omega, \nu) \int_{-\infty}^{\infty} \int_{-\infty}^{\infty} \left| M(\omega, \nu) - \frac{1}{v} F(\omega, \nu) U(\omega, \nu) \right|^2 d\omega d\nu \tag{12}$$

where ω and ν denote the spatial frequencies in the x and y directions respectively and $M(\omega, \nu)$, $F(\omega, \nu)$ and $U(\omega, \nu)$ are the 2-dimensional Fourier transforms of $m(x, y)$, $f(x, y)$ and $u(x, y)$, so that, for example,

$$M(\omega, \nu) = \int_{-\infty}^{\infty} \int_{-\infty}^{\infty} m(x,y) \mathrm{e}^{-\mathrm{i}\omega x} \mathrm{e}^{-\mathrm{i}\nu y} dxdy \tag{13}$$

For a given target profile, $m(x, y)$, the required mass distribution can be achieved by choosing $U(\omega, \nu)$ such that

$$U(\omega, \nu) = \frac{vM(\omega, \nu)}{F(\omega, \nu)} \tag{14}$$

Given that the spray footprint tends to be a smooth

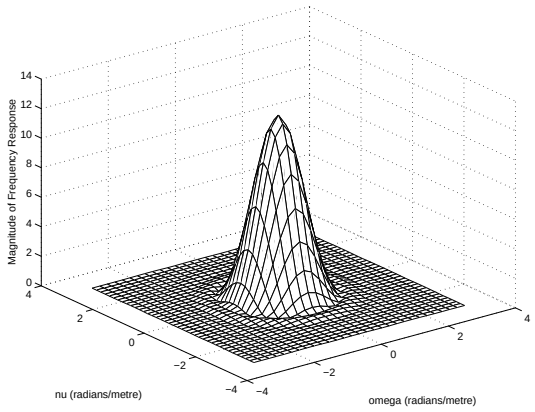

Fig. 4. Magnitude of 2-dimensional Fourier transform of spray footprint in (2)

function, $F(\omega, \nu)$ tends to be bandlimited, in the sense that $|F(\omega, \nu)| < \epsilon$, for some small $\epsilon > 0$ and for all $\omega^2 + \nu^2 \geq \omega_B^2$, where ω_B is the bandwidth. Strictly, for a spatially limited response, such as the one shown in Fig. 2, the Fourier transform of the spatial response cannot also be bandlimited. However, in practice, the spatial responses tend to be smooth and as a result, the magnitude of the frequency response approaches zero rapidly [5]. This is illustrated in Fig. 4, which shows the magnitude of the Fourier transform of the spray footprint shown in Fig. 2 and it can be seen that this response effectively bandlimited around 2 rad/m, although there are some small components of the response outside this value.

For a bandlimited response, $U(\omega, \nu)$ can be chosen so that $F(\omega, \nu)U(\omega, \nu)$ matches $vM(\omega, \nu)$ over the frequency range $\omega^2 + \nu^2 < \omega_B^2$. Because $U(\omega, \nu)$ does not contain frequency components above ω_B, it will also be bandlimited. This means that the underlying mass flow rate function, $u(x, y)$, can be sampled in 2-dimensions without aliasing, provided that the Nyquist frequency of the sampling exceeds ω_B. In principle, the desired mass distribution could be produced by an array of individual, static, evenly-spaced applicators, provided that the applicators are placed sufficiently closely to avoid aliasing. However, in this paper, we are considering a single, moving applicator following the raster pattern, as shown in Fig. 3. Because the short

perpendicular sections between the scans are outside the part being sprayed, when the applicator is on these sections, the sprayed material does not contribute to the overall mass distribution. As a result, each raster can be extended to $\pm\infty$, as shown by the dashed lines in Fig. 3. Under these circumstances, each scan can be considered as a 1-dimensional sample of an underlying 2-dimensional function, $u_b(x, y)$ [8]. The Fourier transform of this sampled signal consists of the Fourier transform of the unsampled signals, $U_b(\omega, \nu)$, repeated in the frequency direction perpendicular to the scan direction [4]. For example, if the parallel scans are all taken in the y direction, as in Fig. 3, the Fourier transform of the rastered $u(x, y)$ can be written as

$$U(\omega, \nu) = \frac{1}{d} \sum_{k=-\infty}^{\infty} U_b(\omega + k\omega_r, \nu) \tag{15}$$

where $\omega_r = 2\pi/d$, with d being the distance between scans. Since $F(\omega, \nu)$ is bandlimited, then $F(\omega, \nu)U(\omega, \nu) = F(\omega, \nu)U_b(\omega, \nu)$, provided that the distance between scans is sufficiently small, so that $\omega_r/2 > \omega_B$, or equivalently,

$$d < \frac{\pi}{\omega_B} \tag{16}$$

This means that the applicator flow rate can be determined by setting

$$U_b(\omega, \nu) = d\frac{vM(\omega, \nu)}{F(\omega, \nu)} \tag{17}$$

over the region $\omega^2 + \nu^2 < \omega_B^2$ and then sampling the inverse Fourier transform, $u_b(x, y)$, along parallel scans whose separation, d, satisfies (16).

The condition in (16) on the separation between the raster scans, is the well-known result from Shannon's sampling theorem [4]. By choosing d such that half the sampling frequency exceeds the bandwidth of the Fourier transform of the applicator's footprint, aliasing is avoided. If this condition is not met, then the effect of aliasing on the resulting mass distribution is to introduce a "ripple" at a frequency close to the Nyquist frequency. The analysis shows that the maximum distance between scans depends upon the bandwidth of the spatial response of the applicator's footprint and also that there is no benefit in reducing the spacing between rasters beyond the largest value of d that satisfies (16). A similar result has been derived for the spacing of the actuators in the cross-directional system used on processes such as paper making and plastic film extrusion [7] and for processing signals obtained from scanning gauges [8].

IV. EXAMPLES

A. Flat Mass Profile

In the majority of applications, the aim is to produce an even mass profile so that $m(x, y) = C$ over the surface, where C is a constant. This corresponds to requiring that $M(\omega, \nu) = C\delta(\omega, \nu)$, and from (14), choosing

$$U_b(\omega, \nu) = d\frac{vC}{F(0, 0)}\delta(\omega, \nu) \tag{18}$$

where $F(0, 0)$ is the d.c. component of $F(\omega, \nu)$, ensures that $M(\omega, \nu) = F(\omega, \nu)U(\omega, \nu)$. If the applicator follows a raster pattern, where the scans are made parallel to the $y-$axis, then the Fourier transform of the sampled signal is

$$U(\omega, \nu) = \sum_{k=-\infty}^{\infty} \frac{vC}{F(0, 0)}\delta(\omega + k\omega_r, \nu) \tag{19}$$

which consists of a series of equally spaced, delta functions arranged along the ω axis, where the distance between the delta functions is $\omega_r = 2\pi/d$. This corresponds to a mass flow rate, $u(x, y)$ that is constant along each of the passes over the surface, so a series of raster sweeps at a constant flow rate, will produce an even distribution of mass, provided that $\omega_r/2 > \omega_B$.

The analysis above was based upon the idealised assumption that both the desired profile, $m(x, y)$ and the raster scans had infinite extent. This assumption can be removed by noting that in practice, the applicator's footprint has finite extent. For example, for the footprint given in (2), there is no mass deposited outside the spray cone, as specified by γ, the half angle of the spray cone. Once the centre of footprint is is a distance, denoted by β, beyond the edge of the surface, it does not deposit any material, so scan can be truncated and the applicator direction reversed, as shown in Fig. 3.

Remark 1. The requirement that $\omega_r/2 > \omega_B$ applies for a general target profile, $m(x, y)$, where $U(\omega, \nu)$ can have the same bandwidth as $F(\omega, \nu)$. For the special case of $m(x, y) = C$, so that $M(\omega, \nu)$ consists of a delta function a the origin, $U(\omega, \nu)$ is also a delta function and aliasing between raster scans will still be avoided if the separation between scans is increased until $d < 2\pi/\omega_B$.

Remark 2. In [12], [13], optimal scanning patterns for generating an even mass deposition are described that require the scan velocity of the applicator to be adjusted. However, these patterns start at the corner of the surface being sprayed and as a result, the velocity needs to be adjusted to overcome the "edge effect". If the applicator's path can be extended so that it sprays outside the edge, as in Fig. 3, then an even mass deposition is achieved with constant applicator velocity and constant mass deposition rate.

The time that the applicator spends between raster scans, where it is spraying outside the part, is wasteful and a number of path planning methods have been used to optimise this portion of the path. An alternative approach is to note that the frequency domain analysis given in this paper does not only apply to raster scans where the applicator moves in a direction parallel to the $y-$axis, but is valid for equally spaced, parallel scans in any direction. Fig. 5 shows a path that is the combination of two separate raster patterns with equally spaced scans, one at an angle $+\psi$ to the $y-$axis and the other at an angle $-\psi$. Each of these raster patterns generates an even mass distribution, so the combined effect of the two patterns also creates an

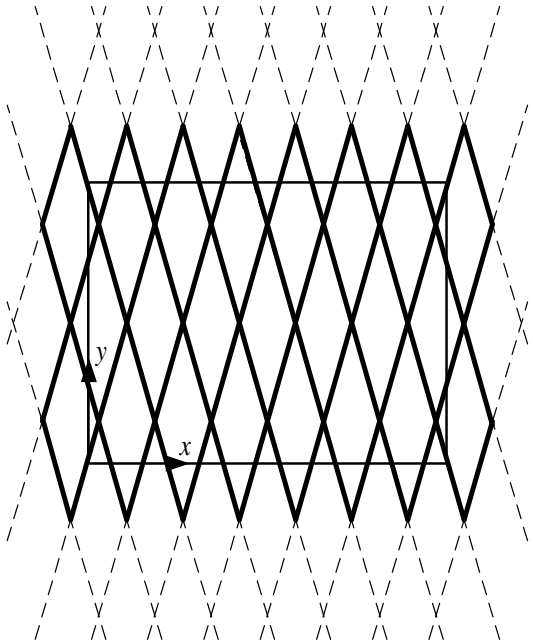

Fig. 5. Spray pattern consisting of the combination of two raster patterns at $\pm\psi$ to the $y-$axis

even distribution. The advantage of this pattern is that it joins the individual raster scans without having to include short sections of path to join up the scans.

B. Shaped Mass Profile

Fig. 6 shows a non-uniform target for the mass distribution, $m(x, y)$, that consists of a dome in the centre of the surface of area 0.4m by 0.3m. Using (17), the underlying mass flow rate profile, $u_b(x, y)$ for a robot velocity of 1 m s^{-1}, is shown in Fig. 7. It can be seen that for this case, the flow rate function does not follow target profile exactly, due to the scaling of $M(\omega, \nu)$ by $F(\omega, \nu)$ in (17). If the flow rate profile is then sampled, using the raster pattern in Fig. 3 where the distance between rasters is $d = 0.031$m, which satisfies (16), then the resultant profile deposited by the applicator is shown in Fig. 8. It can be seen that this matches the required distribution in Fig. 6 well and the maximum absolute value of the error between the required distribution and the actual profile is less that 0.1%. By contrast, if the distance between the rasters is increased so that $d = 0.051$m, for which $d > \pi/\omega_B$, then aliasing occurs, which as shown in Fig. 9 has the effect of introducing a "ripple" with a frequency close to the Nyquist sampling frequency, ω_B. The presence of these ripples increases the maximum absolute error to 8.7%.

Fig. 10 shows the profile generated when the robot follows the angled pattern in 5 where the passes over the surface are at an angle of $\pm 52.7^o$ to the x-axis and the distance between the tracks is $d = 0.019$m. It can be seen that this robot path produces the required mass profile with very small error (less than 0.1%) and as pointed out above, is an efficient way of spraying the part as it minimises the time that the robot spends off the sprayed surface.

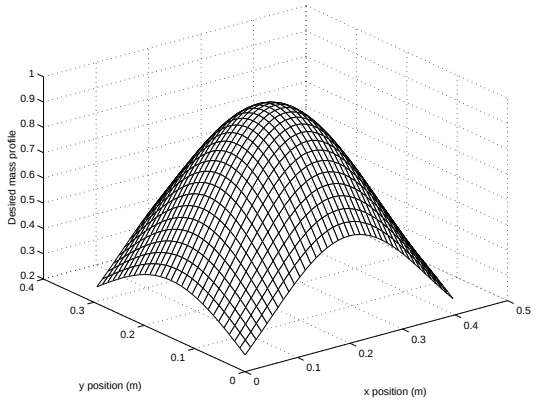

Fig. 6. Target mass distribution profile

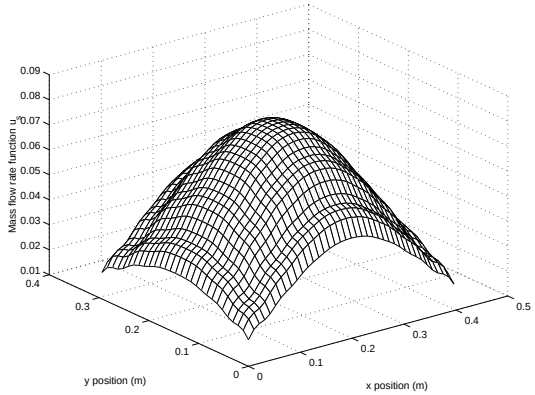

Fig. 7. Flow rate function, $u_b(x, y)$, required to generate target profile in Fig. 6

V. CONCLUSION

This paper has considered the design of robot paths for automated spray deposition processes. Usually, the choice of robot path has been determined by solving an optimisation problem in the spatial domain, but in this paper, the problem is transferred to the spatial frequency domain by applying results from sampling theory. Considering the path planning problem in the frequency domain provides insight into the relationship between the separation between the individual paths. The paper also shows how angled, raster patterns can be combined to provide a continuous path over the surface that generates the required distribution of deposited material.

REFERENCES

[1] J.K. Antonio. Optimal trajectory planning for spray coating. In *Proc. IEEE Int. Conf. on Robotics and Automation*, pages 2570–2577, San Diego, CA, 1994.

[2] J.K. Antonio, R. Ramabhadran, and T.-L. Ling. A framework for optimal trajectory planning for automated spray coating. *International Journal of Robotics and Automation*, 12(4):124–134, 1997.

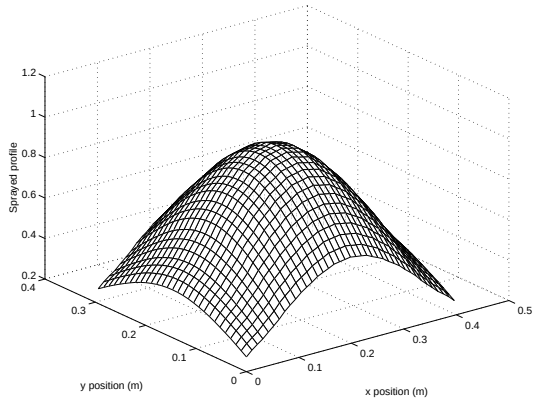

Fig. 8. Resultant mass distribution from applying mass flow rate function in Fig. 7 using raster pattern where raster separation is $d = 0.031\text{m}$

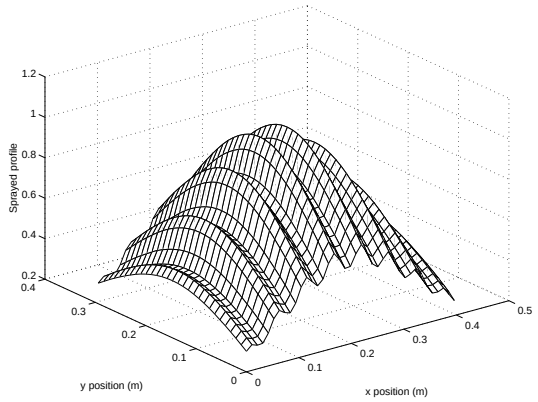

Fig. 9. Resultant mass distribution from applying mass flow rate function in Fig. 7 using raster pattern where raster separation is increased to $d = 0.051\text{m}$

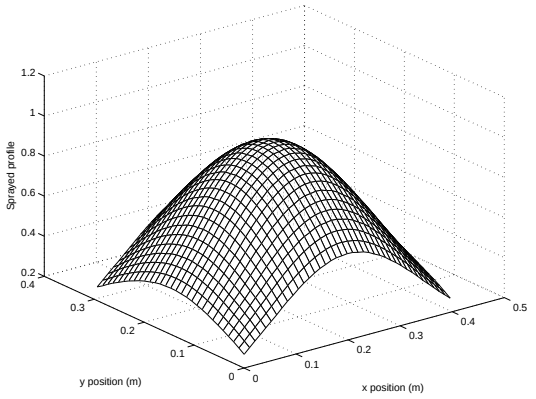

Fig. 10. Resultant mass distribution from applying mass flow rate function in Fig. 7 using an angled raster pattern as shwon in Fig. 3, where the rasters are at an angle of $\pm 52.7^o$ to the x-axis and the raster separation is $d = 0.019\text{m}$

[3] B. Bidanda, V. Narayanan, and J. Rubinovitz. Computer-aided-design-based interactive off-line programming of spray-glazing robots. *Int. J. Computer Integrated Manufacture*, 6:357–365, 1993.

[4] R.N. Bracewell. *The Fourier Transform and its Applications*. McGraw Hill, New York, NY, 2nd edition, 1986.

[5] D.C. Champeney. *A Handbook of Fourier Theorems*. Cambridge University Press, Cambridge, UK, 1987.

[6] Z. Djuric and P.S. Grant. An inverse problem in modelling liquid metal spraying. *Applied Math. Modelling*, 27(5):379–396, 2003.

[7] S.R. Duncan and G.F Bryant. Spatial controllability of cross-directional control systems for web processes. *Automatica*, 33(2):139–153, 1997.

[8] S.R. Duncan and P.E. Wellstead. Processing data from scanning gauges on industrial web processes. *Automatica*, 40:431–437, 2004.

[9] D.M. Hensinger, A.L. Ames, and J.L. Kuhlmann. Motion planning for a direct metal deposition rapid prototyping system. In *Proc. IEEE Int. Conf. on Robotics and Automation*, pages 3095–3100, San Fransico, CA, 2000.

[10] P. Hertling, L. Hog, R. Larsen, J. Perram, and H.G. Petersen. Task curve planning for painting robots - Part 1: process modeling and calibration. *IEEE Transactions on Robotics and Automation*, 12(2):324–330, 1996.

[11] A.J. Jerri. The shannon sampling theorem - its various extensions and applications: a tutorial review. *Proc. IEEE*, 65(11):1565–1595, 1977.

[12] R. Ramabhadran and J.K. Antonio. Planning spatial paths for automated spray coating applications. In *Proc. IEEE Int. Conf. on Robotics and Automation*, pages 1255–1260, Minneapolis, MN, 1996.

[13] R. Ramabhadran and J.K. Antonio. Fast solution techniques for a class of optimal trajectory planning problems with applications to automated spray coating. *IEEE Transactions on Robotics and Automation*, 13(4):519–530, 1997.

[14] W. Sheng, N. Xi, M. Song, Y. Chen, and P. MacNeville. Automated CAD-guided robot path planning for spray painting of compund surfaces. In *Proc. IEEE/RSJ Int. Conf. Intelligent Robots and Systems*, pages 1918–1923, 2000.